▌ **Metallocenes**

Diphosphanylmetallocenes of Main-Group Elements

Carsten Müller, Joshua Warken, Volker Huch, Bernd Morgenstern, Inga-Alexandra Bischoff, Michael Zimmer, and André Schäfer*[a]

Abstract: Several 1,1′-diphosphanyl-substituted metallocenes of magnesium (magnesocenes) were synthesized, structurally characterized, and their reactivity and coordination chemistry were investigated. Transmetalation of these magnesocenes gives access to group 14 metallocenes (tetrelocenes), as well as to group 15 stibonocenes. These s- and p-block metallocenes represent a novel class of bis(phosphanyl) ligands, exhibiting Lewis-amphiphilic character. Their coordination chemistry towards different transition-metal and main-group fragments was investigated and different complexes are presented.

Introduction

Phosphines are one of the most important classes of ligands in coordination chemistry throughout the periodic table, owing to their strong σ-donor abilities.[1] Within this class, bidentate ligands in the form of bis(phosphanyl) compounds are widely recognized for their strong binding capabilities owing to the chelate effect.[2a] Modification of the linker between the phosphanyl groups in these bis(phosphines) can have a strong effect on the bite angle, which is of great importance with regards to steric and electronic properties, and thus for applications in coordination chemistry and catalysis.[2b,c] Within this area, 1,1′-diphosphanyl-substituted ferrocenes have developed into a special class of metal-containing redox active ligands, which have been applied for a variety of transition-metal fragments, since their introduction in the late 1960s.[3] The most prominent examples, 1,1′-bis(diphenylphosphanyl)ferrocene, **dppf**, and the 1,1′-bis(diisopropylphosphanyl)ferrocene, **dippf**, are widely recognized for their applications in homogeneous catalysis, for instance, in the form of palladium or platinum complexes, which, nowadays, are even commercially available.[3d,e]

Furthermore, 1,1′-diphosphanyl-substituted metallocenes of other transition metals are also known, for instance, of lanthanum, yttrium, titanium, zirconium, hafnium, niobium, ruthenium, osmium, cobalt,[4] and in addition, of the lanthanoids europium and ytterbium,[5] as well as of a handful of main-group metals[6] (Figure 1). In some cases, weak interactions between the metallocene central atom and P-complexed metal fragments can be observed, which can be important to the reactivity of these complexes.[3c, 4l, 7] In addition, structurally related heteroleptic complexes of other phosphanyl-functionalized π-ligands like cycloheptatrienyl or phenyl are also known and possess an intriguing coordination chemistry.[8]

As there are several diphosphanyl-substituted metallocenes beyond ferrocenes, mostly exhibiting diphenylphosphanyl or diisopropylphosphanyl groups, a convenient nomenclature for these compounds would be valuable. We suggest to use the popular "dpp" and "dipp" abbreviations for metallocenes possessing a 1,1′-bis(diphenylphosphanyl) or a 1,1′-bis(diisopropylphosphanyl) substitution pattern, derived from the corresponding ferrocene acronyms **dppf** and **dippf**, and combining it with the element symbol. Following this principle, the 1,1′-bis(diphenylphosphanyl)ferrocene, **dppf**, could also be referred to as **dppFe**. This becomes more useful for metallocenes of other metals, for instance, the aforementioned titanium, zirconium, cobalt, and ytterbium species could be referred to as **dppTiCl₂**, **dppZrCl₂**, **dppCo**, and **dppYb**. In addition, the octamethyl derivatives exhibiting permethylated Cp rings can be denoted by a superscript hash, like in the case of tetramethyl-cyclopentadienide, Cp#, and pentamethylcyclopentadienide, Cp*, thus 1,1′-bis(diphenylphosphanyl)octamethyl ferrocene[9] could be abbreviated **dpp#Fe**.

As mentioned above, the concept of 1,1′-diphosphanyl-functionalization is limited to a few main-group metallocenes and remains only sparsely explored, aside from dimethylplatinum complexes of thf-adducts of **dppCa**, **dppSr**, and **dppBa**,[6b] and a gold(I) complex of **dppTl⁻**.[10] This is surprising, as s- and p-block based diphosphanyl-substituted metallocenes present particularly interesting ligands, as the central atom is Lewis-acidic.[11, 12] Therefore, these metallocenes can be regarded as

[a] C. Müller, J. Warken, Dr. V. Huch, Dr. B. Morgenstern, I.-A. Bischoff, Dr. M. Zimmer, Dr. A. Schäfer
Faculty of Natural Sciences and Technology, Department of Chemistry
Saarland University, Campus Saarbrücken, 66123 Saarbrücken (Germany)
E-mail: andre.schaefer@uni-saarland.de

Chemistry–A European Journal

Full Paper
doi.org/10.1002/chem.202005198

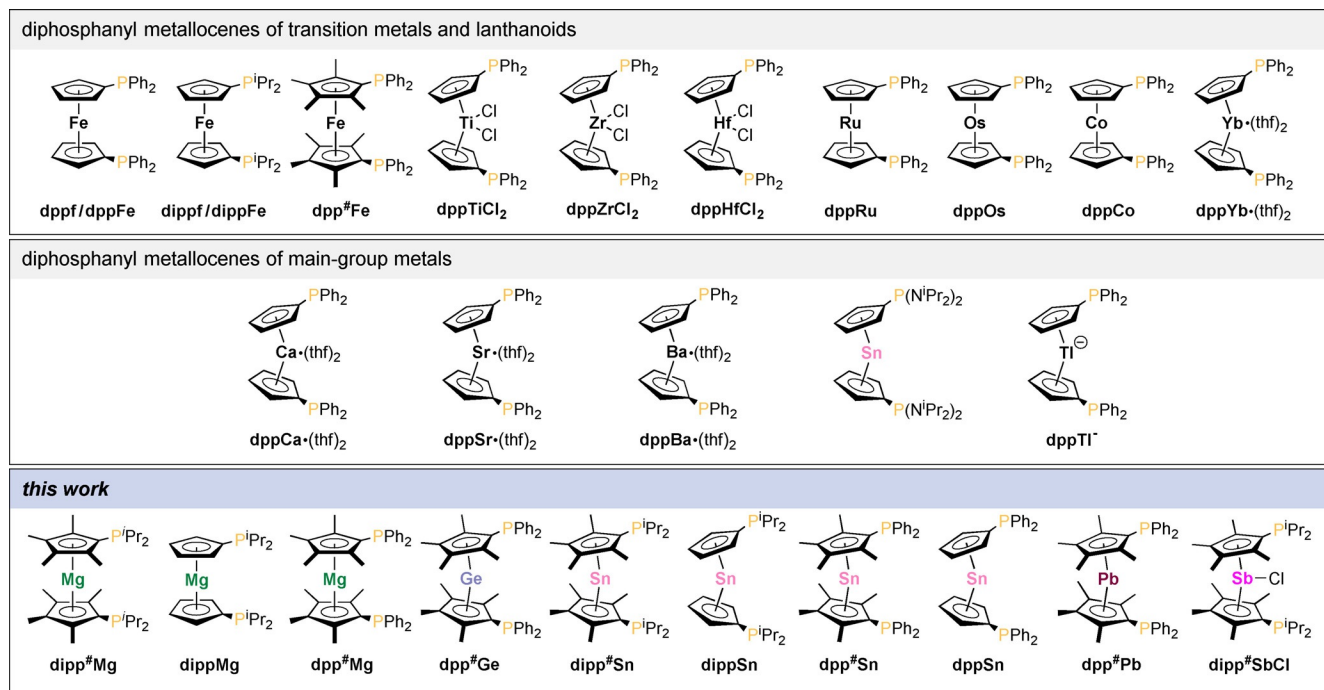**Chemistry Europe**
European Chemical
Societies Publishing

Figure 1. Selected examples of 1,1'-diphosphanyl-substituted metallocenes.

Lewis-amphiphilic ligand systems, with a hard, electron-poor and a soft, electron-rich center.[6b] In general, Lewis-amphiphilic ligands, often based on boron or aluminium, have attracted much attention for their coordination properties, but the use of alkaline earth metals or group 14 elements as Lewis-acidic centers in such ligands is almost unexplored.[13] It should be noted that, so far, the group 2 metallocenes **dppCa**, **dppSr**, and **dppBa**, have only been isolated in the form of their thf adducts in which their Lewis-acidity is quenched by the coordination of the thf molecules.[6b] As group 14 metallocenes (tetrelocenes) are tetrylene-type compounds, and tetrylene complexes of main-group and transition metals have been studied extensively,[14] and following our group's continuous interest in main-group metallocenes, we were intrigued to study diphosphanyl-substituted metallocenes of s- and p-block metals.
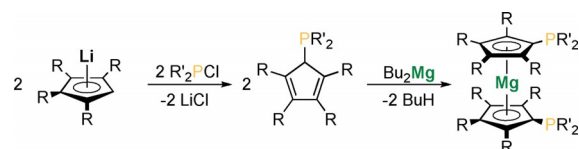
Herein, we report the synthesis and structure of different diphosphanylmagnesocenes **1a–c**, tetrelocenes, **2**, **3a–c**, **4**, and stibonocenes **5a,b** and present a study of their reactivity towards σ-donors, small molecules, and various metal fragments.

Results and Discussion

Magnesocenes

Diphosphanylmagnesocenes **1a–c** (**dipp#Mg**, **dippMg**, **dpp#Mg**) were synthesized by the reaction of lithium cyclopentadienide or lithium tetramethylcyclopentadienide with the corresponding chlorophosphines and subsequent treatment with dibutylmagnesium (Scheme 1).

Magnesocenes **1a–c** are obtained as highly air-sensitive, colorless solids in acceptable to good yields (**1a**: 38%; **1b**: 86%; **1c**: 76%). Notably, the synthesis of a 1,1'-bis(diphenylphospha-

Scheme 1. Synthesis of diphosphanylmagnesocenes **1a–c**. **1a**: R=Me; R'=iPr. **1b**: R=H; R'=iPr. **1c**: R=Me; R'=Ph.

nyl)magnesocene, **1d** (**dppMg**), failed, presumably owing to the instability of the protonated ligand Ph_2PCpH.[15] Compounds **1a–c** show a high degree of solubility in aliphatic and aromatic solvents such as hexane, benzene, and toluene, and were characterized by multinuclear NMR spectroscopy in solution and single-crystal X-ray diffraction analysis in the solid state (Figure 1). In solution, the ^{31}P NMR chemical shifts of **1a–c**, which range from −2.8 to −25.5 ppm depending on the substitution pattern, are in line with known diphosphanylferrocenes ($\delta^{31}P(\textbf{dppFe}) = -16.6$ ppm;[16] $\delta^{31}P(\textbf{dippFe}) = 0.9$ ppm[16]). Notably, **1b** (**dippMg**), exists as a dimer in the solid state (Figure 2a), owing to its Lewis-amphiphilic nature, although magnesocene phosphine complexes have previously been described as unisolable in pure form.[17] The intermolecular Mg–P distances are 274.32(1) pm and 279.45(1) pm, which are longer than in known phosphorous magnesium complexes[18–20] (($\textbf{dppmfluMg}(\mu\text{-}n\text{Bu}))_2$: 262.71(7) pm (dppmflu = $(Ph_2PCH_2PPh_2)$fluorene)). However, with just a few examples of phosphine-coordinated diorgano-substituted magnesium compounds known,[18–20] and no examples of magnesocene phosphine complexes,[17] this value must be assessed carefully. As only a single signal is observed in the $^{31}P\{^1H\}$ NMR spectrum in solution at room temperature, we assume that it is a rather
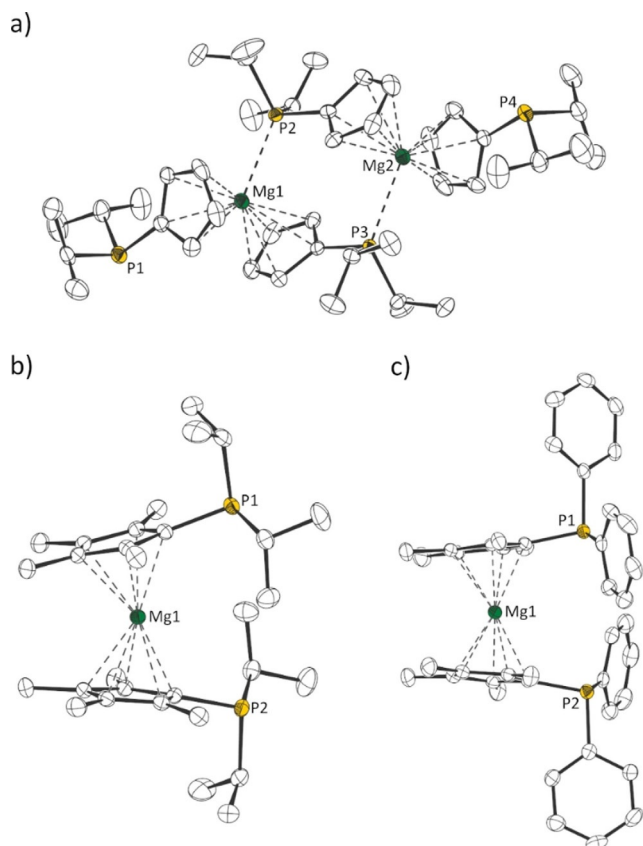
Chemistry–A European Journal

Full Paper
doi.org/10.1002/chem.202005198

**Chemistry
Europe**
European Chemical
Societies Publishing

Table 1. Selected bond lengths, angles, and ^{31}P NMR shifts of **1a–c**, **1b·(thf)₂**, **1b·(CS₂)₂**, **1b·PhNCO**, and **1b·PtMe₂**.

Compound	Mg–Cp[a] [pm]	Cp-Mg-Cp[b] [°]	δ ^{31}P [ppm]
1a (dipp#Mg)	201.36(2)	159.790(5)	−3.8[c]
1b (dippMg)	211.62(1) 213.39(1) 220.60(1)	136.627(3) 135.317(3)	−2.8[c]
1c (dpp#Mg)	198.66(3) 199.05(3)	166.539(11)	−25.5[c]
1b·(thf)₂	224.05(2) 234.57(2) 248.95(1)	–	−2.3[c]
1b·(CS₂)₂	215.39(8)	136.611(2)	36.2[c]
1b·PhNCO	218.16(8) 241.50(2) 282.70(2)	–	24.0 −12.6[d]
1b·PtMe₂	197.34(6) 198.57(6)	164.409(32)	21.0 ($^1J_{PPt}$ = 1862 Hz)[c]

[a] Corresponding to the bonding mode of the Cp ligand. [b] Corresponding to Cp^{cent} and only given in the case of η⁵ bonding. [c] C_6D_6, 162 MHz, 298 K. [d] CP-MAS (13 kHz), 162 MHz, 296 K.
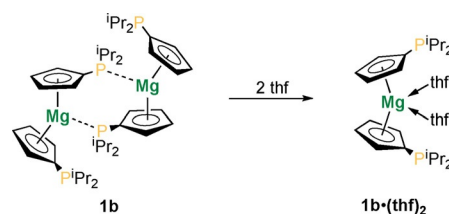
Figure 2. Molecular structures of (a) **1b**-dimer, (b) **1a**, and (c) **1c** in the crystal (displacement ellipsoids at the 50% probability level; H atoms omitted). Selected bond lengths [ppm] and angles [°]: **1b**: Mg1–P2 274.32(1), Mg2–P3 279.45(1), Cp^{cent}–Mg1 211.62(1)/213.39(1)/220.60(1), Cp^{cent}–Mg2 218.36(1)/211.62(1); Cp^{cent}-Mg1-Cp^{cent} 136.627(3), Cp^{cent}-Mg2-Cp^{cent} 135.317(3); **1a**: Cp^{cent}–Mg1 201.36(2); Cp^{cent}-Mg1-Cp^{cent} 159.790(5); **1c**: Cp^{cent}–Mg1 198.66(3)/199.05(3); Cp^{cent}-Mg1-Cp^{cent} 166.539(11).

weak interaction and **1b** (**dippMg**) exists in rapid equilibrium with a monomer in solution. As mentioned above, this is in line with previous reports that the isolation of phosphine adducts of magnesocene failed owing to dissociation in solution.[17] The Mg–Cp distances are shorter in case of the permethylated magnesocenes **1c** (**dpp#Mg**) (198.66(3) pm and 199.05(3) pm) and **1a** (**dipp#Mg**) (201.36(2) pm) and longer in the case of **1b** (**dippMg**) (211.62(1) pm and 220.60(1) pm). This can be attributed to steric and electronic factors, as permethylated Cp rings are more electron rich, resulting in stronger Mg–Cp bonds, and on the other hand, phosphine coordination to the magnesium atom in dimer **1b** increases the electron density and steric pressure on the magnesium atom, which weakens the Mg–Cp bonds. The Cp^{cent}-Mg-Cp^{cent} angles in magnesocenes **1a–c** also differ significantly (Table 1). Only a slight bending is observed for **1c** (**dpp#Mg**) (166.5°) and **1a** (**dipp#Mg**) (159.8°), whereas a strong bending is observed in dimeric **1b** (**dippMg**) (135.3° and 136.6°). This highlights the flexibility of the Mg–Cp bonds, owing to their high ionic character. The previously reported diphosphanyl-metallocenes of calcium, **dppCa·(thf)₂**, strontium, **dppSr·(thf)₂**, and barium, **dppBa·(thf)₂**, are monomeric in the solid state, which is a con-

sequence of the coordination of thf molecules to the central atom.[6b] This prompted us to investigate the reactivity of **1b** (**dippMg**) towards thf. As expected, when dissolved in thf, the corresponding bis(thf) adduct, **1b·(thf)₂**, is obtained in quantitative yields (Scheme 2).

Scheme 2. Reaction of **1b** with thf.

In the solid state, **1b·(thf)₂** exhibits one η⁵- and one η²-bonded Cp ligand (Figure 3). Ring slippage of Cp ligands in the solid state is not uncommon for magnesium Cp compounds and is not reflected by NMR spectroscopy in solution. For example, **1b·(thf)₂** gives only a single resonance in the ^{31}P NMR spectrum ($\delta^{31}P$ = −2.3 ppm) in solution, along with two resonances for Cp protons in the ^1H NMR spectrum. Similar structures have been reported before, for instance, in the case of a magnesocene bis(thf) adduct[21] and also for [1]magnesocenophane bis(thf) adducts.[22]

The Mg–O bond lengths in **1b·(thf)₂** are 206.17(2) pm and 208.14(1) pm, comparable to what is found in $Cp_2Mg·(thf)_2$ (208.8 pm and 209.8(2) pm).[21] The Mg–C bond lengths to the

Chemistry–A European Journal

Full Paper
doi.org/10.1002/chem.202005198

Chemistry Europe
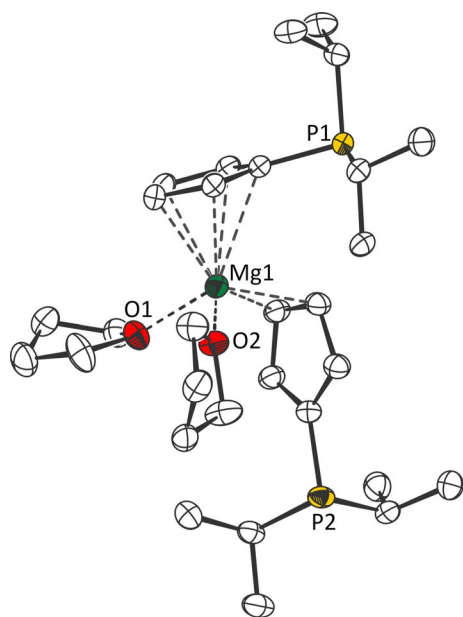European Chemical
Societies Publishing

Figure 3. Molecular structure of **1b·(thf)₂** in the crystal (displacement ellipsoids at the 50% probability level; H atoms omitted). Selected bond lengths [ppm]: Mg1–O1 208.14(1), Mg1–O2 206.17(2), Cp^{cent}–Mg1 224.05(2).

η^2-coordinated Cp ligand are 234.57(2) pm and 248.95(1) pm, suggesting a tendency towards η^1, and the Mg–Cp^{cent} distance to the η^5-bonded Cp moiety is 224.05(2) pm. Inspection of the frontier orbitals of diphosphanylmagnesocene **1b** (**dippMg**) (Figure 4) highlights its Lewis-amphiphilic character.

HOMO and HOMO−1 exhibit large coefficients at the phosphorus atoms, corresponding to the lone pairs. In comparison, the LUMO is predominantly localized on the magnesium atom, highlighting its Lewis-acidic character. The Lewis-amphiphilicity of **1b** (**dippMg**) prompted us to study its reactivity not only towards metal fragments, but also towards small/organic molecules, as such molecules can often be activated and coordinated by Lewis-amphiphilic frustrated Lewis pair (FLP)-type systems.[24] Indeed, treatment of solutions of **1b** (**dippMg**) with carbon disulfide and phenyl isocyanate, led to formation of the corresponding adducts (Scheme 3). In the case of the CS₂ complex, a downfield shifted doublet in the ¹³C{¹H} NMR spectrum at 237.0 ppm (J_{CP} = 37 Hz) was detected, which is comparable to other CS₂ phosphorous adducts.[24a]
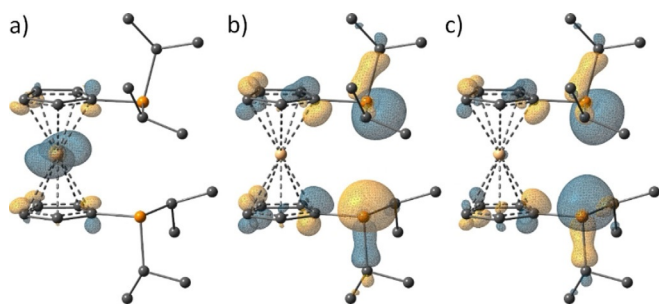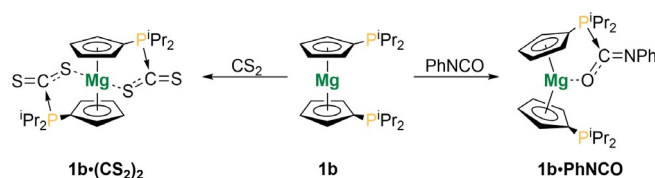

Figure 4. Isosurface plots of (a) LUMO, (b) HOMO, and (c) HOMO−1 of magnesocene **1b** (B3LYP-D3/def2-TZVP,[23] isovalue = 0.05).

Scheme 3. Reaction of **1b** with CS₂ and PhNCO.

To the best of our knowledge, **1b·(CS₂)₂** is the first example of a magnesium CS₂ complex of this kind. In the solid state (Figure 5), **1b·(CS₂)₂** possesses two η^5-coordinated Cp ligands. The P–C bonds in **1b·(CS₂)₂** are 183.71(124) pm, which is almost identical to Sn/P and B/P FLP CS₂ complexes[24a,c] ((Fxyl)₂BCH₂PtBu₂·CS₂: 183.5(8) pm; (F₅C₂)₃SnCH₂PtBu₂·CS₂: 184.7(2) pm), whereas the Mg–S bonds are 249.48(39) pm, which is longer than in a related magnesium dithiocarbonate complex,[24d] but shorter than in a dithiobenzoate complex.[24e] Remarkably, **1b** (**dippMg**) does not undergo a Mg–C insertion reaction with CS₂, in contrast to what is common for Grignard reagents.[24e] Similar to **1b** (**dippMg**), **1b·PhNCO** exhibits a dimeric structure in the solid state[25] with Mg–P bonds of 256.23(1) pm and 273.70(1) pm (Figure S79 in the Supporting Information). The bonding situation of the Cp ligands in **1b·PhNCO** in the solid state is best regarded as η^5 and η^2, like in the afore-discussed bis(thf) adduct **1b·(thf)₂**. The Mg–O bond length is 195.65(1) pm, which is slightly shorter than in other magnesium phenyl isocyanate complexes[26] ([(Me₄TACD)Mg·PhNCHO]⁺: 204.3(6) pm (TACD = tetraazacyclododecane)). On the other hand, the P–C bond is 184.80(18) pm, which is slightly shorter than in related FLP complexes of phenyl isocyanate[24c] ((F₅C₂)₃SnCH₂PtBu₂·PhNCO: 185.0(2) pm). In solution at room temperature, several signals are observed in the ³¹P NMR spectrum upon dissolving the crystals of **1b·PhNCO** in benzene-D₆, presumably owing to decomposition of the complex. In the ³¹P{¹H} CP-MAS NMR spec-
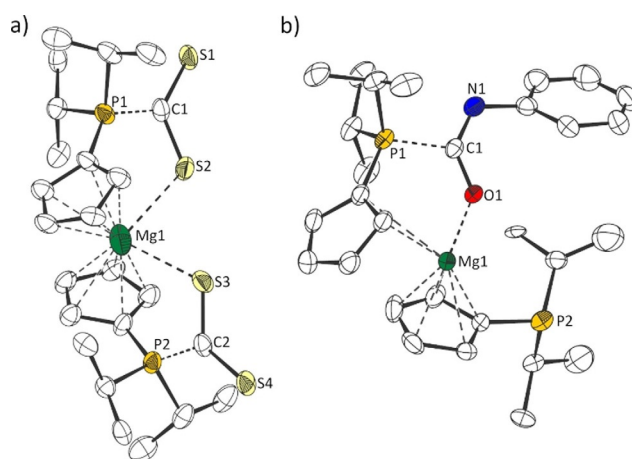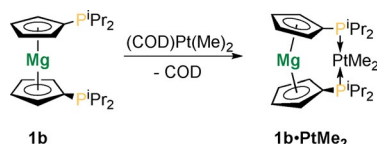

Figure 5. Molecular structure of (a) **1b·(CS₂)₂** and (b) **1b·PhNCO** in the crystal (displacement ellipsoids at the 50% probability level; H atoms omitted). Selected bond lengths [ppm] and angles [°]: **1b·(CS₂)₂**: Mg1–S2/S3 249.48(39), Cp^{cent}–Mg1 215.39(8), P1–C1/P2–C2 183.71(124); Cp^{cent}-Mg1-Cp^{cent} 136.611(2); **1b·PhNCO**: Mg1–O1 195.65(1), P1–C1 184.80(18), Cp^{cent}–Mg1 218.16(8).

Chemistry–A European Journal

Full Paper
doi.org/10.1002/chem.202005198

Chemistry Europe
European Chemical
Societies Publishing

trum of **1b·PhNCO**, two signals are observed, as one would expect.[25] To assess the bonding energy of phenyl isocyanate to the magnesocene moiety in complex **1b·PhNCO**, we performed DFT calculations at the B3LYP-D3/def2-TZVP level of theory,[23] which suggest a complexation energy of 135.4 kJ mol^{-1}.

It has previously been shown that diphosphanyl-substituted metallocenes of heavy group 2 metals can be used as ligands in platinum complexes. This is particularly interesting, as these ligand systems have highly variable bite angles, owing to the ionic character of the alkaline earth metal Cp bonds. Noteworthy, the reported complexes, **dppCa·(thf)$_2$·PtMe$_2$**, **dppSr·(thf)$_2$·PtMe$_2$**, **dppBa·(thf)$_2$·PtMe$_2$**, all exhibited two thf molecules bound to the group 2 metal. No solvent-free complexes of alkaline earth metals and no complexes of magnesium had previously been described. When (COD)PtMe$_2$ is added to a toluene solution of **1b** (**dippMg**), immediate precipitation of the product **1b·PtMe$_2$** as a colorless solid is observed (Scheme 4), which was obtained in 75% yield.

Scheme 4. Reaction of **1b** with (COD)Pt(Me)$_2$.

Compound **1b·PtMe$_2$** is an example of an early–late hetero-bimetallic complex (ELHB), which have been discussed intensively for their applications in catalysis.[27] Platinum complex **1b·PtMe$_2$** shows a signal at 21.0 ppm in the ^{31}P NMR spectrum, with a platinum coupling of $^1J_{PPt} = 1862$ Hz (Table 1). This is similar to **dppCa·(thf)$_2$·PtMe$_2$** ($^1J_{PPt} = 1878$ Hz[6b]) and **dppFe·PtMe$_2$** ($^1J_{PPt} = 1903$ Hz[28]), and typical for *cis*-bis(phosphine) complexes of dimethylplatinum(II).[29] Notably, in contrast to the previously reported platinum complexes of heavier group 2 diphosphanyl metallocenes,[6b] **1b·PtMe$_2$** can be isolated without solvent coordination to the central atom (Figure 6),
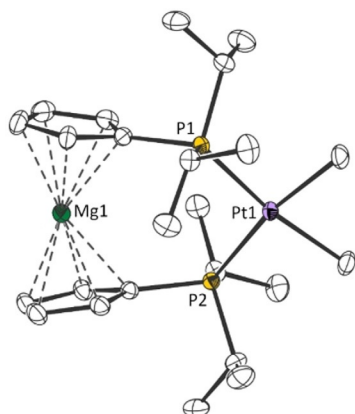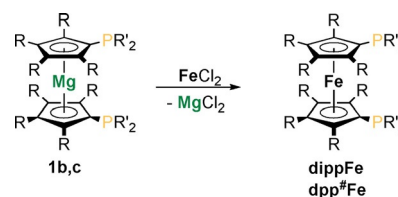
Figure 6. Molecular structure of **1b·PtMe$_2$** in the crystal (displacement ellipsoids at the 50% probability level; H atoms omitted). Selected bond lengths [ppm] and angles [°]: P1–Pt1 231.19(4), P2–Pt1 232.73(4), Cp^{cent}–Mg1 197.34(6)/198.57(6); Cp^{cent}-Mg1-Cp^{cent} 164.409(32), P1-Pt1-P2 105.129(13).

retaining the Lewis-acidity of the magnesium atom. The P–Pt bonds in **1b·PtMe$_2$** measure 231.19(4) pm and 232.73(4) pm in the solid state, comparable to those of **dppCa·(thf)$_2$·PtMe$_2$** (229.00(7) pm and 229.15(7) pm).
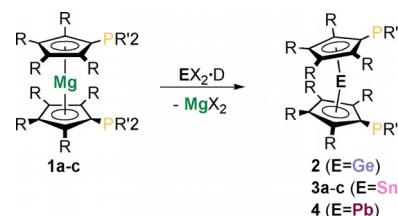
As magnesium Cp compounds are known to be excellent Cp-transfer reagents, we probed the possibility to synthesize other diphosphanylmetallocenes starting from magnesocenes **1a–c**. In the first instance, as proof of concept, we reacted **1b,c** with iron(II) chloride and were able to obtain the corresponding ferrocenes (Scheme 5).[25] Although **dippFe** can more easily be obtained by dilithiation and functionalization of ferrocene, this route is a useful approach for the synthesis of **dpp#Fe**.

Scheme 5. Transmetalation of **1b,c** with iron(II) chloride (**dippFe**: R = H, R' = *i*Pr; **dpp#Fe**: R = Me, R' = Ph).

Tetrelocenes

Following the successful synthesis of ferrocenes **dippFe** and **dpp#Fe** starting from magnesocenes **1b,c**, we were able to prepare diphosphanyltetrelocenes **2** (**dpp#Ge**), **3a–c** (**dipp#Sn**, **dippSn**, **dpp#Sn**), and **4** (**dpp#Pb**) by transmetalation of **1a–c** with the corresponding group 14 dichlorides in acceptable to good yields (Scheme 6).

Scheme 6. Synthesis of **2**, **3a–c**, and **4** by transmetalation of **1a–c** with the corresponding group 14 element dichlorides. **2**: R = Me; R' = Ph. **3a**: R = Me; R' = *i*Pr. **3b**: R = H; R' = *i*Pr. **3c**: R = Me; R' = Ph. **3d**: R = H; R' = Ph. **4**: R = Me; R' = Ph.

Bis(diphenylphosphanyl)stannocene, **3d** (**dppSn**), of which the corresponding magnesocene (**dppMg**) could not be prepared, could be obtained in 1% yield by a reaction sequence starting from lithium cyclopentadienide.[25] In contrast to magnesocene **1b** (**dippMg**), stannocene **3b** (**dippSn**) exhibits a monomeric structure in the crystal, just like all diphosphanyltetrelocenes, **2**–**4**, (Figures 7 and 8). This highlights the decreasing Lewis-acidity of the tetrels compared with magnesium.

The Cp^{cent}-E-Cp^{cent} angles decrease from germanocene **2** (**dpp#Ge**) to stannocene **3c** (**dpp#Sn**) to plumbocene **4** (**dpp#Pb**). This trend, going from lighter to heavier group 14 el-
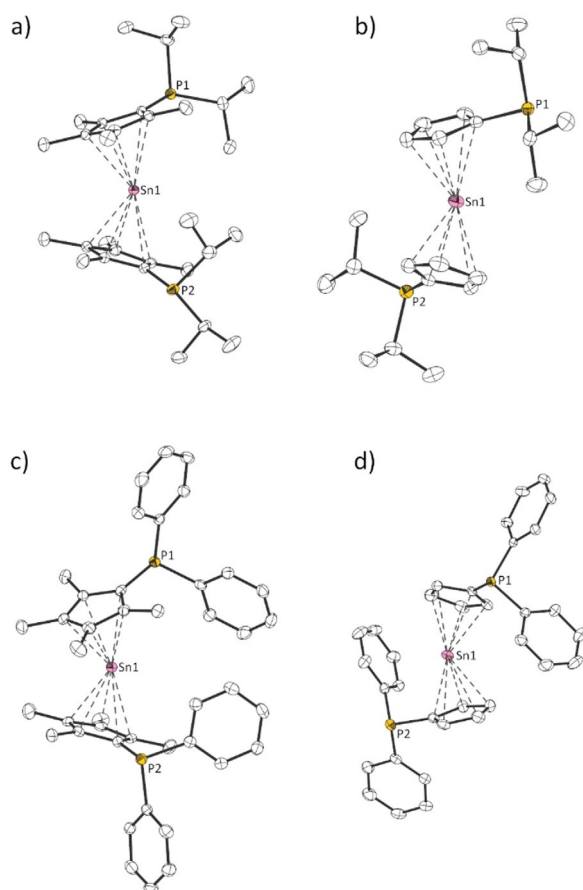
Chemistry–A European Journal

Full Paper
doi.org/10.1002/chem.202005198

Chemistry Europe
European Chemical
Societies Publishing

Figure 7. Molecular structures of (a) **3 a**, (b) **3 b**, (c) **3 c**, and (d) **3 d** in the crystal (displacement ellipsoids at the 50% probability level, H atoms omitted). Selected bond lengths [ppm] and angles [°]: **3 a**: Cp^{cent}–Sn1 237.67(1)/240.43(1); Cp^{cent}-Sn1-Cp^{cent} 156.147(3), **3 b**: Cp^{cent}–Sn1 240.39(1)/242.21(1); Cp^{cent}-Sn1-Cp^{cent} 152.593(2); **3 c**: Cp^{cent}–Sn1 240.93(1)/242.09(1); Cp^{cent}-Sn1-Cp^{cent} 152.753(3); **3 d**: Cp^{cent}–Sn1 242.92(1)/242.93(1); Cp^{cent}-Sn1-Cp^{cent} 146.951(4).
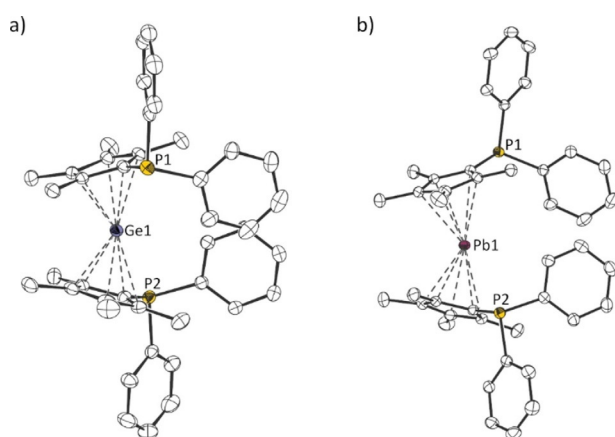

Figure 8. Molecular structures of (a) **2** and (b) **4** in the crystal (displacement ellipsoids at the 50% probability level; H atoms omitted). Selected bond lengths [ppm] and angles [°]: **2**: Cp^{cent}–Ge1 220.20(3)/222.33(3); Cp^{cent}-Ge1-Cp^{cent} 159.932(15); **4**: Cp^{cent}–Pb1 247.82(2)/249.19(2); Cp^{cent}-Pb1-Cp^{cent} 150.575(11).

Cp^{cent}–E bond lengths increase from **2** to **3 c** to **4**, which is in line with the increasing size of the central atom. It is noteworthy that **2** (**dpp#Ge**) is the first example of a diphosphanylmetalloidocene, a diphosphanyl-substituted metallocene-type compound based on a metalloid element. Benzene-D$_6$ solutions of diphosphanyltetrelocenes, **2**–**4**, show similar ^{31}P resonance of −4.8 to −28.7 ppm as magnesocenes **1 a**–**c** (Tables 1 and 2), and corresponding ferrocenes[16,30] (δ^{31}P(**dppFe**) = −16.6 ppm; δ^{31}P(**dippFe**) = 0.9 ppm; δ^{31}P(**dpp#Fe**) = −20.1 ppm). The ^{119}Sn NMR chemical shifts of diphosphanyl-stannocenes **3 a**–**d** range from −2134 ppm to −2199 ppm (Table 2), which is similar to stannocene[31] (δ^{119}Sn(Cp$_2$Sn) = −2199 ppm) and decamethyl-stannocene[31] (δ^{119}Sn(Cp*$_2$Sn) = −2129 ppm). Diphosphanylplumbocene **4** (**dpp#Pb**) shows a single ^{207}Pb resonance at −4668 ppm, which is in line with other plumbocenes[31] (δ^{207}Pb(Cp$_2$Pb) = −5030 ppm; δ^{207}Pb(Cp*$_2$Pb) = −4390 ppm).

Inspection of the frontier orbitals of **3 b** (**dippSn**) shows that the HOMO and HOMO−1 correspond predominantly to the lone pairs of the phosphorus atoms, whereas the LUMO is almost exclusively located on the tin atom in the shape of a p-orbital, suggesting that this compound has Lewis-amphiphilic character. The lone pair on the tin atom in the form of the HOMO−7 is comparably low in energy and of high s-character (Figure 9).[12] Qualitatively identical frontier orbitals can be found in all diphosphanyltetrelocenes, **2**–**4**.

To investigate whether **3 b** (**dippSn**) does indeed possess Lewis-amphiphilic reactivity as suggested by the frontier orbitals, we reacted it with a σ-donor in the form of an N-heterocyclic carbene (NHC), as well as with different Lewis-acidic metal fragments. We have previously shown that stannocenes can form isolable complexes with different NHCs.[12d] In line with this, stannocene **3 b** (**dippSn**) forms a stable carbene complex,

ements, is a result of decreasing hybridization and less lone-pair character on the central atom. On the other hand, the

Table 2. Selected bond lengths, angles, ^{31}P, ^{119}Sn, and ^{207}Pb NMR shifts of **2**, **3 a**–**d**, **4**.

Compound	E–Cp[a] [pm]	Cp-E-Cp[a] [°]	δ ^{31}P[b] [ppm]	δ ^{119}Sn[c]/ δ ^{207}Pb[d] [ppm]
2 (**dpp#Ge**)	220.20(3) 222.33(3)	159.932(15)	−27.4	–
3 a (**dipp#Sn**)	237.67(1) 240.43(1)	156.147(3)	−4.9	−2176
3 b (**dippSn**)	240.39(1) 242.21(1)	152.593(2)	−4.8	−2134
3 c (**dpp#Sn**)	240.93(1) 242.09(1)	152.753(3)	−27.5	−2199
3 d (**dppSn**)	242.92(1) 242.93(1)	146.951(4)	−22.6	−2197
4 (**dpp#Pb**)	247.82(2) 249.19(2)	150.575(11)	−28.7	−4668

[a] Corresponding to Cp^{centroid}. [b] C$_6$D$_6$, 162 MHz, 298 K. [c] C$_6$D$_6$, 149 MHz, 298 K. [d] C$_6$D$_6$, 63 MHz, 298 K.

Chemistry–A European Journal

Full Paper
doi.org/10.1002/chem.202005198

Chemistry Europe
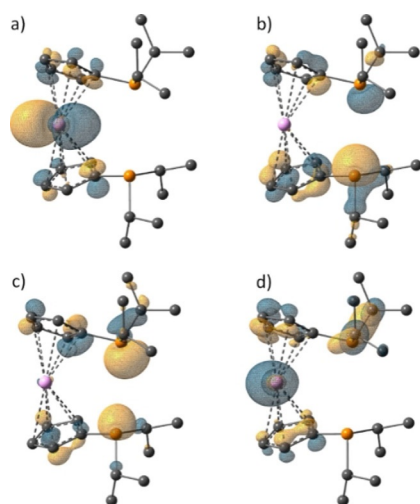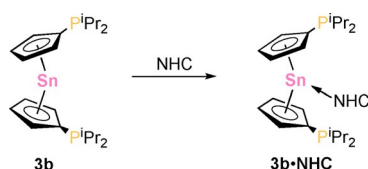European Chemical
Societies Publishing

Figure 9. Isosurface plots of (a) LUMO, (b) HOMO, (c) HOMO−1, and (d) HOMO−7 of **3 b** (B3LYP-D3/def2-TZVP;[23] isovalue = 0.05).

3 b·NHC, with 1,3-diisopropyl-4,5-dimethylimidazolin-2-ylidene (Scheme 7).

In **3 b·NHC**, the NHC is side-on coordinated to the metallocene moiety (Figure 10), similar to previously reported stannocene complexes.[12d] The Cp^{cent}—Sn bond lengths (259.31(1) pm and 264.86(1) pm) are significantly elongated compared with **3 b** (240.39(1) pm and 242.21(1) pm) and the Cp^{cent}-Sn-Cp^{cent} angle of **3 b·NHC** (134.8°) is smaller than in **3 b** (**dippSn**) (152.6°), as a result of the NHC coordination. Compound **3 b·NHC** clearly highlights the Lewis-acidic character of the tin atom in **3 b** (**dippSn**).

Scheme 7. Reaction of **3 b** with NHC (NHC = 1,3-diisopropyl-4,5-dimethyl-imidazolin-2-ylidene).
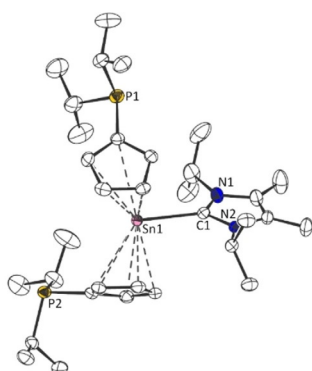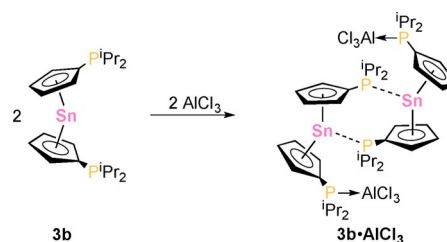

Figure 10. Molecular structure of **3 b·NHC** in the crystal (displacement ellipsoids at the 50% probability level, H atoms omitted). Selected bond lengths [ppm] and angles [°]: Sn1—C1 241.63(0), Cp^{cent}—Sn1 259.31(1)/264.86(1); Cp^{cent}-Sn1-Cp^{cent} 134.767(1).

To probe the applicability of **3 b** (**dippSn**), as a ligand, we reacted it with aluminium(III) chloride, and were able to obtain a corresponding adduct, **3 b·AlCl₃**, in 52% yield (Scheme 8).

The solid-state structure reveals that aluminium complex **3 b·AlCl₃** possesses a dimeric structure in the solid state (Figure 11 a), owing to the Lewis-acidity of the tin center, which is remarkable as **3 b** (**dippSn**) itself is monomeric in the solid state and phosphine complexes of stannocenes are unknown. Accordingly, **3 b·AlCl₃** is the first example of a structurally characterized phosphine adduct of a tetrelocene, and in general, phosphine complexes of stannylenes are extremely rare. The Sn—P distance of 298.78(2) pm is significantly longer than in other phosphine complexes of diaryl- or disilylstannylenes[32,33] (TerSn-μ-aceNaph(PiPr₂): 263.62(6) pm (Ter = 2,6-bis(2,4,6-triisopropylbenzene)xylene, aceNaph = 1,2-dihydroacenaphthylene); (Me₂Si(SiMe₃)₂Si)₂Sn(PEt₃): 260.8(3) pm). The solid-state structure is, however, not persistent in solution at room temperature, as only one set of isopropyl groups is observed in the ^{1}H and ^{13}C{^{1}H} NMR spectra, accompanied by broad signals in the ^{27}Al{^{1}H} (δ^{27}Al = 111.2 ppm; $\nu_{1/2}$ = 121 Hz) and ^{31}P{^{1}H} NMR spectra (δ^{31}P = −7.5 ppm; $\nu_{1/2}$ = 25 Hz), along with a single resonance in the ^{119}Sn{^{1}H} NMR spectrum (δ^{119}Sn = −2172 ppm), suggesting that the dimeric structure is not maintained in solution but that both phosphorus atoms are equivalent, possibly owing to a fast coordination isomerism. The reaction of stannocene **3 b** (**dippSn**) with 2 equivalents of aluminium(III) chlo-

Scheme 8. Reaction of **3 b** with 1 equivalent of AlCl₃.
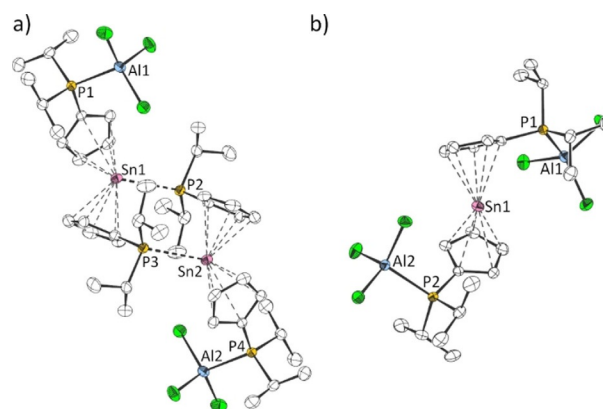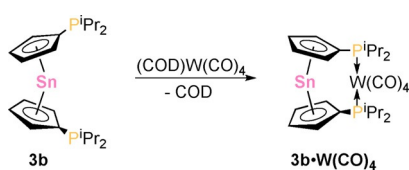

Figure 11. Molecular structures of (a) **3 b·AlCl₃** dimer and (b) **3 b·(AlCl₃)₂** in the crystal (displacement ellipsoids at the 50% probability level; H atoms omitted). Selected bond lengths [ppm] and angles [°]: **3 b·AlCl₃**: Sn1—P2/ Sn2—P3 298.78(2), P1—Al1/P4—Al2 240.41(1), Cp^{cent}—Sn1/Cp^{cent}—Sn2 254.00(1)/255.93(1); Cp^{cent}-Sn1-Cp^{cent}/Cp^{cent}-Sn2-Cp^{cent} 130.684(2); **3 b·(AlCl₃)₂**: P1—Al1 242.47(1), P2—Al2 240.69(0), Cp^{cent}—Sn1 242.09(0)/242.45(0); Cp^{cent}-Sn1-Cp^{cent} 145.535(1).

Scheme 9. Reaction of **3b** with 2 equivalents of $AlCl_3$.

ride yields **3b·(AlCl₃)₂**, where both phosphorus atoms are bound to an $AlCl_3$ moiety (Scheme 9, Figure 11 b).

A solution of **3b·(AlCl₃)₂** in C_6D_6, exhibits one broad signal in $^{31}P\{^1H\}$ NMR ($\delta^{31}P = -12.2$ ppm; $\nu_{1/2} = 283$ Hz) and $^{27}Al\{^1H\}$ NMR spectrum ($\delta^{27}Al = 110.9$ ppm; $\nu_{1/2} = 189$ Hz), along with only one signal in the $^{119}Sn\{^1H\}$ NMR spectrum ($\delta^{119}Sn = -2178$ ppm). The Al—P bonds in **3b·AlCl₃** and **3b·(AlCl₃)₂** are very similar (**3b·AlCl₃**: 240.41(1) pm; **3b·(AlCl₃)₂**: 240.69(0) pm and 242.47(1) pm) and are in line with $AlCl_3·PMe_3$[34] (239.2(2) pm). In **3b·NHC**, the Lewis-acidic character of the tin atom of **3b** (**dippSn**) is indicated, whereas in **3b·(AlCl₃)₂** the Lewis-basicity of the phosphorus atoms is indicated, and especially in **3b·AlCl₃** the Lewis-basic and acidic character are highlighted, displaying the Lewis-amphoterism of **3b** (**dippSn**).

Following these results, we investigated the reactivity of germanocene **2** (**dpp#Ge**) and stannocene **3b** (**dippSn**) towards different transition-metal fragments. As tetrelocenes in general usually exhibit flexible bent structures with free rotation around the E—Cp bonds owing to a certain degree of ionic character, diphosphanyltetrelocenes have highly variable bite angles, unlike many transition-metal analogs. Therefore, they should be adaptable to different metal fragments. In this regard, the 14-electron tetracarbonyltungsten(0) fragment proved to be a suitable candidate for a stable stannocene complex. When stannocene **3b** (**dippSn**) was reacted with $(COD)W(CO)_4$, the corresponding complex **3b·W(CO)₄** was obtained (Scheme 10).

Scheme 10. Reaction of **3b** with $(COD)W(CO)_4$.

The ^{31}P NMR chemical shift of **3b·W(CO)₄** is observed at 13.4 ppm with ^{183}W satellites with a coupling constant of $^1J_{PW} = 229$ Hz, similar to $1,4-(Ph_2P)_2(C_4H_8)·W(CO)_4$[35b] ($^1J_{PW} = 228.5$ Hz). Remarkably, as a solid, **3b·W(CO)₄**, proved to be air stable for at least 2 h, exemplified by its 18-electron configuration. In the solid state (Figure 12), the tungsten atom reveals a distorted octahedral coordination geometry, with the two phosphorus atoms in *cis*-positions in the equatorial plane, and consequently two CO ligands in *cis*-positions in the equatorial plane and two in the axial positions. The P—W bond lengths of 258.78(20) pm and 259.21(21) pm (Table 3) are similar to
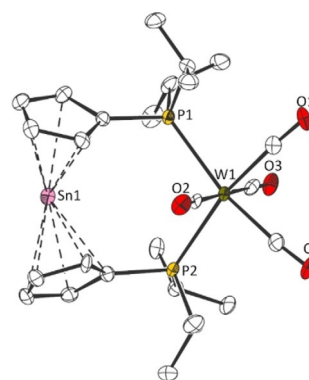

Figure 12. Molecular structure of **3b·W(CO)₄** in the crystal (displacement ellipsoids at the 50% probability level; H atoms omitted). Selected bond lengths [ppm] and angles [°]: P1—W1 259.21(21), P2—W1 258.78(20), Cp^{cent}—Sn1 238.89(6)/241.09(6); Cp^{cent}-Sn1-Cp^{cent} 139.308(26), P1-W1-P2 107.498(65).

Table 3. Selected bond lengths, angles, ^{31}P and ^{119}Sn NMR shifts of complexes **2·PtMe₂**, **3b·NHC**, **3b·AlCl₃**, **3b·(AlCl₃)₂**, **3b·PtMe₂**, and **3b·W(CO)₄**.
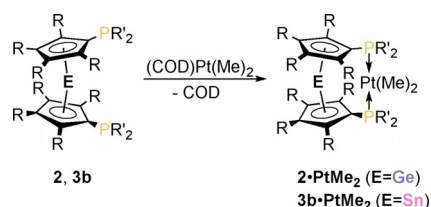
Compound	E—Cp[a] [pm]	Cp-E-Cp[a] [°]	P-M-P [°]	δ ^{31}P[b] [ppm]	δ ^{119}Sn[c] [ppm]
2·PtMe₂	219.77(1) 220.17(1)	162.993(2)	107.338(2)	19.6 ($^1J_{PPt} = 2011$ Hz)	–
3b·NHC	259.31(1) 264.86(1)	134.767(1)	–	−4.7	–
3b·AlCl₃	254.00(1) 255.93(1)	130.684(2)	–	−7.5	−2172
3b·(AlCl₃)₂	242.09(0) 242.45(0)	145.535(1)	–	−12.2	−2178
3b·PtMe₂	237.30(2) 243.11(2)	149.810(4)	105.935(4)	22.0 ($^1J_{PPt} = 1843$ Hz)	−2170
3b·W(CO)₄	238.89(6) 241.09(6)	139.308(26)	107.498(65)	13.4 ($^1J_{PW} = 229$ Hz)	−2176

[a] Corresponding to $Cp^{centroid}$. [b] C_6D_6, 162 MHz, 298 K. [c] C_6D_6, 149 MHz, 298 K.

dppFe·W(CO)₄[36] (253.32(16) pm and 256.27(17) pm). Interestingly, the P-W-P bite angle in **3b·W(CO)₄** is 107.5°, which is significantly larger than what is found in comparable compounds[35a,b, 36] (**dppFe·W(CO)₄**: 95.2°; $[o-(iPr_2P)_2(C_6H_4)]·W(CO)_4$: 79.8° and 80.1°; $1,4-(Ph_2P)_2(C_4H_8)·W(CO)_4$: 91.7°), thus a surprisingly large bite angle and strong deviation from an ideal 90° angle.

As shown before, magnesocene **1b** (**dippMg**) could be utilized as a ligand for dimethylplatinum(II). To investigate analogous complexes with group 14 metallocene ligands, germanocene **2** (**dpp#Ge**) and stannocene **3b** (**dippSn**) were reacted with $(COD)PtMe_2$ to give the corresponding complexes **2·PtMe₂** and **3b·PtMe₂** (Scheme 11).

Chemical shifts in the $^{31}P\{^1H\}$ NMR spectra of 19.6 ppm (**2·PtMe₂**) and 22.0 ppm (**3b·PtMe₂**) with coupling constants of $^1J_{PPt} = 2011$ Hz (**2·PtMe₂**) and $^1J_{PPt} = 1843$ Hz (**3b·PtMe₂**; Table 3)

Chemistry–A European Journal

Full Paper
doi.org/10.1002/chem.202005198

Chemistry Europe
European Chemical
Societies Publishing

Scheme 11. Reaction of **2** and **3 b** with (COD)Pt(Me)$_2$.

are similar to magnesium complex **1 c·PtMe₂** and **dppFe·PtMe₂** (see above). The ^{119}Sn NMR chemical shift of **3 b·PtMe₂** (δ^{119}Sn = −2170 ppm) is upfield shifted by $\Delta\delta^{119}$Sn = 36 ppm compared with free stannocene **3 b** (**dippSn**).

In the solid-state structures of **2·PtMe₂** and **3 b·PtMe₂**, the platinum atom shows a slightly distorted square-planar coordination geometry (Figure 13), with a P—Pt bond length similar to **dppFe·PtMe₂**[29b] (**2·PtMe₂**: 229.40(1) pm and 229.46(1) pm; **3 b·PtMe₂**: 232.34(2) pm and 232.80(2) pm; **dppFe·PtMe₂**: 229.10(19) pm and 229.48(23) pm), and large P-Pt-P bite angles of 107.3° (**2·PtMe₂**) and 105.9° (**3 b·PtMe₂**), which are much larger than in the iron analog **dppFe·PtMe₂**[29b] (100.8°) and similar to what was observed in tungsten complex **3 b·W(CO)₄**. It is worth mentioning that large bite angles of this sort are often discussed with regards to high catalytic activity, for instance, in hydroformylation reactions involving rhodium complexes with bidentate bis(phosphanyl) ligands.[2b,c]
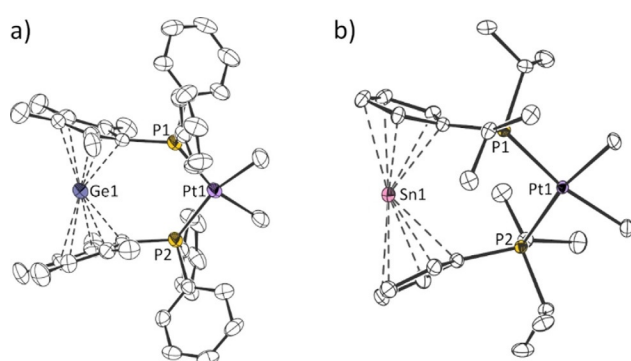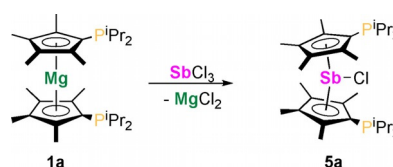

Figure 13. Molecular structures of (a) **2·PtMe₂** and (b) **3 b·PtMe₂** in the crystal (displacement ellipsoids at the 50 % probability level; H atoms omitted). Selected bond lengths [ppm] and angles [°]: **2·PtMe₂**: P1–Pt1 229.40(1), P2–Pt1 229.46(1), Cp^{cent}–Ge1 219.77(1)/220.17(1); Cp^{cent}-Ge1-Cp^{cent} 162.993(2), P1-Pt1-P2 107.338(2); **3 b·PtMe₂**: P1–Pt1 232.80(2), P2–Pt1 232.34(2), Cp^{cent}–Sn1 237.30(2)/243.11(2); Cp^{cent}-Sn1-Cp^{cent} 149.810(4), P1-Pt1-P2 105.935(4).

A stibonocene and stibonocenium cation

Only a few examples of π-bonded cyclopentadienyl compounds of antimony are known, most of which possess bulky Cp ligands such as ((*t*Bu)₃C₅H₂)⁻ and (Me₅C₅)⁻.[37,38] Furthermore, P-functionalized metallocenes of group 15 elements are completely unknown so far. As magnesocenes **1 a–c** have proven to be powerful Cp-transfer reagents in the synthesis of ferrocenes and tetrelocenes, we attempted the synthesis of chlorostibonocene **5 a** (**dipp#SbCl**) starting from magnesocene **1 a** (**dipp#Mg**). Indeed, when magnesocene **1 a** (**dipp#Mg**) is

Scheme 12. Reaction of **1 a** with antimony(III) chloride.

treated with antimony(III) chloride in toluene at 198 K, the corresponding diphosphanylchlorostibonocene **5 a** (**dipp#SbCl**) can be obtained (Scheme 12).

Chlorostibonocene **5 a** (**dipp#SbCl**) represents the first example of a diphosphanylmetallocene-type compound based on a group 15 element. To probe the possibility of preparing a highly Lewis-amphiphilic stibonocenium cation, we reacted equimolar amounts of aluminium(III) chloride and chlorostibonocene **5 a** (**dipp#SbCl**) in a toluene/*ortho*-difluorobenzene mixture, and obtained the stibonocenium aluminate salt, **5 b[AlCl₄]** (**[dipp#Sb][AlCl₄]**) (Scheme 13).

In the solid state (Figure 14), chlorostibonocene **5 a** (**dipp#SbCl**) and stibonocenium cation **5 b** (**dipp#Sb⁺**) both exhibit bent structures with two π-complexed Cp ligands in distorted η⁵-coordination mode, with a tendency towards η³. This is evident from the different Sb–C^{Cp} bond lengths (**5 a**: 259.11(22) pm to 277.68(21) pm; **5 b**: 243.98(17) pm to 275.45(15) pm), although the C^{Cp}–C^{Cp} bond lengths are relatively uniform (**5 a**: 140.08(30) pm to 143.67(29) pm; **5 b**: 141.34(21) pm to 145.25(22) pm), indicating a high degree of π-conjugation. The Cp^{cent}-Sb-Cp^{cent} bending angle is 140.0° in
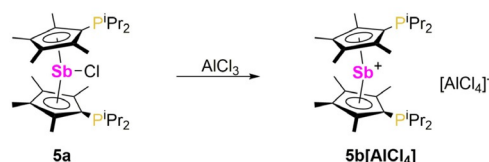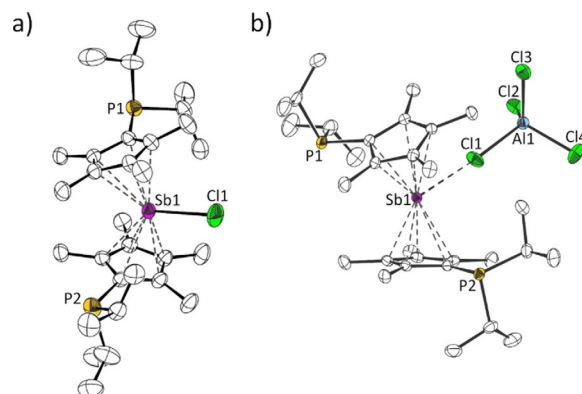

Scheme 13. Reaction of **5 a** with aluminium(III) chloride.

Figure 14. Molecular structures of (a) **5 a** and (b) **5 b[AlCl₄]** in the crystal (displacement ellipsoids at the 50 % probability level; H atoms omitted). Selected bond lengths [ppm] and angles [°]: **5 a**: Sb1–Cl1 257.71(9), Cp^{cent}–Sb1 238.34(3)/239.16(3); Cp^{cent}-Sb1-Cp^{cent} 139.946(11), **5 b[AlCl₄]**: Sb1–Cl1 349.44(5), Cp^{cent}–Sb1 229.63(2)/230.03(3); Cp^{cent}-Sb1-Cp^{cent} 162.346(13).

5a (**dipp#SbCl**) and 162.4° in **5b** (**dipp#Sb+**). Similar structural features are found in Cp*$_2$SbCl and Cp*$_2$Sb+,[37e] and in the tin analog **3a** (**dipp#Sn**). Interestingly, in contrast to [Cp*$_2$Sb][AlCl$_4$][37e] and [Me$_4$Si$_2$[2](C$_5$Me$_4$)$_2$Sb][AlCl$_4$],[37f] which both exhibit two cation–anion Sb–Cl contacts, **5b[AlCl$_4$]** ([**dipp#Sb**][AlCl$_4$]) reveals only one cation–anion Sb–Cl contact, measuring 349.44(5) pm, which is shorter than in the aforementioned salts[37e,f] (374.40(23) pm to 375.99(21) pm), but significantly longer than the Sb–Cl bond in chlorostibonocene **5a** (**dipp#SbCl**) (257.71(9) pm).

Overall, phosphanyl-functionalized metallocenium cations of group 15 elements represent a new and fascinating class of Lewis-amphiphilic compounds, which will be interesting for small molecule binding as well as ligands for transition-metal fragments in the future.

Conclusion

Herein, we describe a series of new phosphanyl-functionalized metallocenes based on main-group elements. Magnesocenes **1a–c** (**dipp#Mg, dippMg, dpp#Mg**) are Lewis-amphiphilic compounds and can be used in small molecule activation, as ligands for transition-metal fragments and as Cp-transfer reagents in the preparation of ferrocenes and group 14 and 15 metallocenes. The first results of our reactivity studies include carbon disulfide complex **1b·(CS$_2$)$_2$**, isocyanate complex **1b·PhNCO**, and platinum complex **1b·PtMe$_2$**. By transmetalation with the corresponding group 14 dichlorides and antimony trichloride, we were able to synthesize a corresponding germanocene **2** (**dpp#Ge**), a series of stannocenes, **3a–d** (**dipp#Sn, dippSn, dpp#Sn, dppSn**), plumbocene **4** (**dpp#Pb**) and the first examples of phosphanyl-functionalized group 15 metallocenes, in the form of chlorostibonocene **5a** (**dipp#SbCl**) and stibonocenium cation **5b** (**dipp#Sb+**). The coordination chemistry of germanocene **2** (**dpp#Ge**) and stannocene **3b** (**dippSn**) was examined and a series of new heterobimetallic complexes with tungsten, platinum, and aluminium fragments could be obtained. In addition, the Lewis-acidity of the tin atom in stannocene **3b** (**dippSn**) is highlighted by the isolation of carbene complex **3b·NHC**.

This work lays the foundation for a new class of main-group metallocene-based bis(phosphanyl) ligands, which possess great potential for future applications as ligands and in different bond-activation processes.

Acknowledgments

Conflict of interest

The authors declare no conflict of interest.

[1] "Phosphines and related P–C-bonded compounds": D. W. Allen in *Organophosphorus Chemistry*, Royal Society of Chemistry, Cambridge, **2011**, pp. 1–51.

[2] a) A. Pascariu, S. Iliescu, A. Popa, G. Ilia, *J. Organomet. Chem.* **2009**, *694*, 3982–4000; b) P. C. J. Kamer, P. W. N. M. van Leeuwen, J. N. H. Reek, *Acc. Chem. Res.* **2001**, *34*, 895–904; c) Z. Freixa, P. W. N. M. van Leeuwen, *Dalton Trans.* **2003**, 1890–1901.

[3] a) J. H. L. Ong, C. Nataro, J. A. Golen, A. L. Rheingold, *Organometallics* **2003**, *22*, 5027–5032; b) S. L. Martinak, L. A. Sites, S. J. Kolb, K. M. Bocage, W. R. McNamara, A. L. Rheingold, J. A. Golen, C. Nataro, *J. Organomet. Chem.* **2006**, *691*, 3627–3632; c) M. R. Ringenberg, *Chem. Eur. J.* **2019**, *25*, 2396–2406; d) S. W. Chien, T. S. A. Hor in *Ferrocenes, Vol. 2* (Ed.: P. Stepnicka), Wiley, Chichester, **2008**, pp. 33–116; e) T. J. Colacot, S. Parisel in *Ferrocenes, Vol. 3* (Ed.: P. Stepnicka), Wiley, Chichester, **2008**, pp. 117–140; f) G. Marr, T. Hunt, *J. Chem. Soc. C* **1969**, 1070–1072; g) J. J. Bishop, A. Davison, M. L. Katcher, D. W. Lichtenberg, R. E. Merrill, J. C. Smart, *J. Organomet. Chem.* **1971**, *27*, 241–249.

[4] a) R. M. Bellabarba, G. P. Clancy, P. T. Gomes, A. M. Martins, L. H. Rees, M. L. H. Green, *J. Organomet. Chem.* **2001**, *640*, 93–112; b) M. Moriya, R. Fröhlich, G. Kehr, G. Erker, S. Grimme, *Chem. Asian J.* **2008**, *3*, 753–758; c) C. Leblanc, C. Moise, A. Maisonnat, R. Poilblanc, C. Charrier, F. Mathey, *J. Organomet. Chem.* **1982**, *231*, C43–C48; d) B. L. Booth, K. G. Smith, *J. Organomet. Chem.* **1981**, *220*, 229–237; e) W. Tikkanen, J. W. Ziller, *Organometallics* **1991**, *10*, 2266–2273; f) A. W. Rudie, D. W. Lichtenberg, M. L. Katcher, A. Davison, *Inorg. Chem.* **1978**, *17*, 2859–2863; g) D. L. DuBois, C. W. Eigenbrot, A. Miedaner, J. C. Smart, R. C. Haltiwanger, *Organometallics* **1986**, *5*, 1405–1411; h) W. Tikkanen, Y. Fujita, J. L. Petersen, *Organometallics* **1986**, *5*, 888–894; i) C. Cornelissen, G. Erker, G. Kehr, R. Fröhlich, *Organometallics* **2005**, *24*, 214–225; j) J. Szymoniak, M. M. Kubicki, J. Besançon, C. Moise, *Inorg. Chim. Acta* **1991**, *180*, 153–160; k) S. Li, B. Wei, P. M. N. Low, H. K. Lee, T. S. A. Hor, F. Xue, T. C. W. Mak, *J. Chem. Soc. Dalton Trans.* **1997**, 1289–1294; l) O. V. Gusev, A. M. Kalsin, P. V. Petrovskii, K. A. Lyssenko, Y. F. Oprunenko, C. Bianchini, A. Meli, W. Oberhauser, *Organometallics* **2003**, *22*, 913–915; m) T. Miyazaki, Y. Tanabe, M. Yuki, Y. Miyake, Y. Nishibayashi, *Organometallics* **2011**, *30*, 2394–2404; n) A. Antiñolo, T. Expósito, I. del Hierro, D. Lucas, Y. Mugnier, I. Orive, A. Otero, S. Prashar, *J. Organomet. Chem.* **2002**, *655*, 63–69.

[5] a) G. B. Deacon, A. Dietrich, C. M. Forsyth, H. Schumann, *Angew. Chem. Int. Ed. Engl.* **1989**, *28*, 1370–1371; *Angew. Chem.* **1989**, *101*, 1374–1375; b) H. Schumann, J. A. Meese-Marktscheffel, B. Gorella, F. H. Görlitz, *J. Organomet. Chem.* **1992**, *428*, C27–C32; c) R. Broussier, G. Delmas, P. Perron, B. Gautheron, J. L. Petersen, *J. Organomet. Chem.* **1996**, *511*, 185–192; d) G. Lin, W.-T. Wong, *J. Organomet. Chem.* **1996**, *523*, 93–98.

[6] a) A. H. Cowley, J. G. Lasch, N. C. Norman, C. A. Stewart, T. C. Wright, *Organometallics* **1983**, *2*, 1691–1692; b) D. P. Daniels, G. B. Deacon, D. Harakat, F. Jaroschik, P. C. Junk, *Dalton Trans.* **2012**, *41*, 267–277.

[7] a) K. M. Gramigna, J. V. Oria, C. L. Mandell, M. A. Tiedemann, W. G. Dougherty, N. A. Piro, W. S. Kassel, B. C. Chan, P. L. Diaconescu, C. Nataro, *Organometallics* **2013**, *32*, 5966–5979; b) E. P. Warnick, R. J. Dupuis, N. A. Piro, W. Scott Kassel, C. Nataro, *Polyhedron* **2016**, *114*, 156–164.

[8] a) L. B. Kool, M. Ogasa, M. D. Rausch, R. D. Rogers, *Organometallics* **1989**, *8*, 1785–1790; b) M. Ogasa, M. D. Rausch, R. D. Rogers, *J. Organomet. Chem.* **1991**, *403*, 279–291; c) S. K. Mohapatra, S. Büschel, C. Daniliuc, P. G. Jones, M. Tamm, *J. Am. Chem. Soc.* **2009**, *131*, 17014–17023; d) H. Braunschweig, M. Drisch, M. Friedrich, T. Kupfer, K. Radacki, *Organometallics* **2011**, *30*, 5202–5207; e) T. R. Eger, I. Munstein, A. Steiner, Y. Sun, G. Niedner-Schatteburg, W. R. Thiel, *J. Organomet. Chem.* **2016**, *810*, 51–56.

[9] G. Trouve, R. Broussier, B. Gautheron, M. M. Kubicki, *Acta Crystallogr. Sect. C* **1991**, *47*, 1966–1967.

[10] G. K. Anderson, N. P. Rath, *J. Organomet. Chem.* **1991**, *414*, 129–135.

[11] a) D. Stalke, *Angew. Chem. Int. Ed. Engl.* **1994**, *33*, 2168–2171; *Angew. Chem.* **1994**, *106*, 2256–2259; b) S. Harder, *Coord. Chem. Rev.* **1998**, *176*, 17–66; c) A. Xia, J. E. Knox, M. J. Heeg, H. B. Schlegel, C. H. Winter, *Organometallics* **2003**, *22*, 4060–4069.

[12] a) M. A. Beswick, N. L. Cromhout, C. N. Harmer, P. R. Raithby, C. A. Russell, J. S. B. Smith, A. Steiner, D. S. Wright, *Chem. Commun.* **1996**, 1977–1978; b) D. R. Armstrong, M. A. Beswick, N. L. Cromhout, C. N. Harmer, D. Moncrieff, C. A. Russell, P. R. Raithby, A. Steiner, A. E. H. Wheatley, D. S. Wright, *Organometallics* **1998**, *17*, 3176–3181; c) M. A. Beswick, J. S. Palmer, D. S. Wright, *Chem. Soc. Rev.* **1998**, *27*, 225–232; d) C. Müller, A. Stahlich, L. Wirtz, C. Gretsch, V. Huch, A. Schäfer, *Inorg. Chem.* **2018**, *57*, 8050–8053; e) L. Wirtz, M. Jourdain, V. Huch, M. Zimmer, A. Schäfer, *ACS Omega* **2019**, *4*, 18355–18360; f) S. Danés, C. Müller, L. Wirtz, V. Huch, T. Block, R. Pöttgen, A. Schäfer, D. M. Andrada, *Organometallics* **2020**, *39*, 516–527.

[13] G. Bouhadir, D. Bourissou, *Chem. Soc. Rev.* **2016**, *45*, 1065–1079.

[14] a) M. Asay, C. Jones, M. Driess, *Chem. Rev.* **2011**, *111*, 354–396; b) J. Baumgartner, C. Marschner, *Rev. Inorg. Chem.* **2014**, *34*, 119–152; c) L. Álvarez-Rodríguez, J. A. Cabeza, P. García-Álvarez, D. Polo, *Coord. Chem. Rev.* **2015**, *300*, 1–28; d) V. Nesterov, D. Reiter, P. Bag, P. Frisch, R. Holzner, A. Porzelt, S. Inoue, *Chem. Rev.* **2018**, *118*, 9678–9842; e) A. Doddi, M. Peters, M. Tamm, *Chem. Rev.* **2019**, *119*, 6994–7112; f) Y. Mizuhata, T. Sasamori, N. Tokitoh, *Chem. Rev.* **2009**, *109*, 3479–3511 [Corrigendum: Y. Mizuhata, T. Sasamori, N. Tokitoh, *Chem. Rev.* **2010**, *110*, 3850]; g) E. Rivard, *Dalton Trans.* **2014**, *43*, 8577–8586.

[15] F. Mathey, J.-P. Lampin, *Tetrahedron* **1975**, *31*, 2685–2690.

[16] T. Sixt, M. Sieger, M. J. Krafft, D. Bubrin, J. Fiedler, W. Kaim, *Organometallics* **2010**, *29*, 5511–5516.

[17] a) R. Benn, H. Lehmkuhl, K. Mehler, A. Rufińska, *Angew. Chem. Int. Ed. Engl.* **1984**, *23*, 534–535; *Angew. Chem.* **1984**, *96*, 521–523; b) R. Benn, A. Rufińska, *Angew. Chem. Int. Ed. Engl.* **1986**, *25*, 861–881; *Angew. Chem.* **1986**, *98*, 851–871; c) H. Lehmkuhl, K. Mehler, R. Benn, A. Rufińska, C. Krüger, *Chem. Ber.* **1986**, *119*, 1054–1069.

[18] A. Pape, M. Lutz, G. Müller, *Angew. Chem. Int. Ed. Engl.* **1994**, *33*, 2281–2284; *Angew. Chem.* **1994**, *106*, 2375–2377.

[19] A. Koch, S. Krieck, H. Görls, M. Westerhausen, *Inorganics* **2016**, *4*, 39.

[20] J. Langer, I. Kosygin, R. Puchta, J. Pahl, S. Harder, *Chem. Eur. J.* **2016**, *22*, 17425–17435.

[21] A. Jaenschke, J. Paap, U. Behrens, *Organometallics* **2003**, *22*, 1167–1169.

[22] a) P. J. Shapiro, S.-J. Lee, P. Perrotin, T. Cantrell, A. Blumenfeld, B. Twamley, *Polyhedron* **2005**, *24*, 1366–1381; b) P. Perrotin, P. J. Shapiro, M. Williams, B. Twamley, *Organometallics* **2007**, *26*, 1823–1826; c) P. Perrotin, B. Twamley, P. J. Shapiro, *Acta Crystallogr. Sect. E* **2007**, *63*, m1277–m1278.

[23] All DFT calculations were performed by using the Gaussian 09 Revision D.01 software suite. See the Supporting Information for further details and references.

[24] a) K. Samigullin, I. Georg, M. Bolte, H.-W. Lerner, M. Wagner, *Chem. Eur. J.* **2016**, *22*, 3478–3484; b) I. G. Albuerne, M. A. Alvarez, M. E. García, D. García-Vivó, M. A. Ruiz, *Dalton Trans.* **2017**, *46*, 3510–3525; c) P. Holtkamp, F. Friedrich, E. Stratmann, A. Mix, B. Neumann, H.-G. Stammler, N. W. Mitzel, *Angew. Chem. Int. Ed.* **2019**, *58*, 5114–5118; *Angew. Chem.* **2019**, *131*, 5168–5172; d) R. Lalrempuia, A. Stasch, C. Jones, *Chem. Sci.* **2013**, *4*, 4383–4388; e) R. Grubba, W. Wojnowski, K. Baranowska, E. Baum, J. Pikies, *Acta Crystallogr. Sect. E* **2006**, *62*, m2080–m2081.

[25] See the Supporting Information for further details.

[26] L. E. Lemmerz, A. Wong, G. Ménard, T. P. Spaniol, J. Okuda, *Polyhedron* **2020**, *178*, 114331.

[27] a) V. Ritleng, M. J. Chetcuti, *Chem. Rev.* **2007**, *107*, 797–858; b) N. Wheatley, P. Kalck, *Chem. Rev.* **1999**, *99*, 3379–3420.

[28] H. R. Shahsavari, M. Rashidi, S. M. Nabavizadeh, S. Habibzadeh, F. W. Heinemann, *Eur. J. Inorg. Chem.* **2009**, 3814–3820.

[29] a) C. M. Haar, S. P. Nolan, W. J. Marshall, K. G. Moloy, A. Prock, W. P. Giering, *Organometallics* **1999**, *18*, 474–479; b) D. C. Smith, C. M. Haar, E. D. Stevens, S. P. Nolan, W. J. Marshall, K. G. Moloy, *Organometallics* **2000**, *19*, 1427–1433.

[30] A. P. Shaw, J. R. Norton, D. Buccella, L. A. Sites, S. S. Kleinbach, D. A. Jarem, K. M. Bocage, C. Nataro, *Organometallics* **2009**, *28*, 3804–3814.

[31] C. Janiak, H. Schumann, C. Stader, B. Wrackmeyer, J. J. Zuckerman, *Chem. Ber.* **1988**, *121*, 1745–1751.

[32] S. Freitag, K. M. Krebs, J. Henning, J. Hirdler, H. Schubert, L. Wesemann, *Organometallics* **2013**, *32*, 6785–6791.

[33] H. Arp, J. Baumgartner, C. Marschner, T. Müller, *J. Am. Chem. Soc.* **2011**, *133*, 5632–5635.

[34] J. Burt, W. Levason, M. E. Light, G. Reid, *Dalton Trans.* **2014**, *43*, 14600–14611.

[35] a) S.-T. Liu, C.-L. Tsao, M.-C. Cheng, S.-M. Peng, *Acta Crystallogr. Sect. C* **1989**, *45*, 1879–1881; b) E. Lindner, R. Fawzi, H. A. Mayer, K. Eichele, W. Hiller, *Organometallics* **1992**, *11*, 1033–1043.

[36] L.-C. Song, J.-T. Liu, Q.-M. Hu, G.-F. Wang, P. Zanello, M. Fontani, *Organometallics* **2000**, *19*, 5342–5351.

[37] a) W. Frank, *J. Organomet. Chem.* **1991**, *406*, 331–341; b) Y. Ehleiter, G. Wolmershäuser, H. Sitzmann, R. Boese, *Z. Anorg. Allg. Chem.* **1996**, *622*, 923–930; c) H. Sitzmann, Y. Ehleiter, G. Wolmershäuser, A. Ecker, C. Üffing, H. Schnöckel, *J. Organomet. Chem.* **1997**, *527*, 209–213; d) M. Schiffer, B. P. Johnson, M. Scheer, *Z. Anorg. Allg. Chem.* **2000**, *626*, 2498–2504; e) R. J. Wiacek, J. N. Jones, C. L. Macdonald, A. H. Cowley, *Can. J. Chem.* **2002**, *80*, 1518–1523; f) A. S. D. Stahlich, V. Huch, A. Grandjean, K. Rohe, K. I. Leszczyńska, D. Scheschkewitz, A. Schäfer, *Chem. Eur. J.* **2019**, *25*, 173–176; g) O. Coughlin, T. Krämer, S. L. Benjamin, *Dalton Trans.* **2020**, *49*, 1726–1730.

[38] a) P. Jutzi, N. Burford, *Chem. Rev.* **1999**, *99*, 969–990; b) P. H. M. Budzelaar, J. J. Engelberts, J. H. van Lenthe, *Organometallics* **2003**, *22*, 1562–1576.